



Anti-site-induced diluted magnetism in semiconductive CoFeTiAl alloy



T.T. Lin ^{a, b}, X.F. Dai ^a, L.Y. Wang ^a, X.T. Wang ^a, X.F. Liu ^c, Y.T. Cui ^b, G.D. Liu ^{a, b, *}

^a School of Material Sciences and Engineering, Hebei University of Technology, Tianjin, 300130, PR China

^b School of Physics and Electronic Engineering, Chongqing Normal University, Chongqing, 400044, PR China

^c Department of Materials Science and Engineering, The University of Tennessee, Knoxville, TN37996, USA

ARTICLE INFO

Article history:

Received 7 July 2015

Received in revised form

11 October 2015

Accepted 16 October 2015

Available online 19 October 2015

Keywords:

Heusler alloy

Diluted magnetic semiconductor

Anti-site

Electronic band structure calculation

ABSTRACT

The spin-polarized electronic band structure calculations are carried out to theoretically investigate the effect of anti-site disordering to the electronic band structure and magnetic properties of LiMgPdSb-type CoFeTiAl alloy. We found that the Co–Ti and Fe–Ti antisite disordering can induce the diluted magnetism in CoFeTiAl alloy. Especially, the Fe–Ti antisite disordering can induce a 100% spin polarization at the Fermi level at a certain degree of anti-site disordering. The Co–Fe antisite disordering is easy to occur in CoFeTiAl alloy but has little effect on the semiconductive characteristic and magnetic properties. The Co, Fe and Ti atoms at the anti-site contribute the magnetization in CoFeTiAl alloy. The diluted magnetism in CoFeTiAl alloy can be induced by the anti-site disordering instead of the introduction of magnetic dopant elements.

© 2015 Elsevier B.V. All rights reserved.

1. Introduction

Heusler alloys have been intensively investigated in both experiment and theory because many attractive materials have been found in these alloys, like half-metal [1], shape memory alloy [2], topological insulator [3] and spin gapless semiconductor [4] etc. Especially, the half-metals are the most suitable materials to many spintronics devices, such as giant magnetoresistance (GMR), tunneling magnetoresistance (TMR) and spin-injecting devices etc. due to their 100% spin-polarization of conductive electrons. However, in practical applications, the lattice mismatch and the electronic mismatch usually lead to the destruction of high spin polarization [5–7]. For example, Bonell et al. [5] demonstrate the strong influence of mismatch dislocations and show that reducing their density strongly enhances the TMR. So, it is required to reduce the mismatch between the semiconductor/normal metal layer and the magnetic material layer as far as possible. The half-metals with Heusler structure are very mismatched to the current typical semiconductors in the lattice and the electronic structure. So, an important work is to search for highly-matched semiconductor and half-metallic materials with Heusler structure. In the past decades,

dozens of highly spin-polarized materials have been found in Heusler alloys, but only a small number of semiconductors were reported. Up to now, the semiconductors with Heusler structure reported are CoTiSb, NiTiSn, CoNbSn [8], Fe₂VAl [9], Fe₂TiSn [10,11] and Fe₂TiSi [12]. The work on these materials is mainly focused on the thermoelectricity and the diluted magnetic properties [13–25].

The ternary Heusler alloys have been investigated massively. Since Dai et al. [26] investigated the electronic structures, crystal structure and magnetic properties of the quaternary CoFeMnSi in 2009, the field of quaternary Heusler alloys has received great attraction by scientific researchers [27–32]. Özdoğan et al. [29] studied dozens of quaternary Heusler alloys and found some half-metals, some spin-gapless semiconductors and some magnetic semiconductors. Zhang et al. [33] calculated the band gap and magnetism of CoFeTiZ (Z = Si, Ge, Sn) alloy and showed that CoFeTiSi and CoFeTiGe alloys are both typically half-metallic ferrimagnets and CoFeTiSn is a quasi-half-metallic ferrimagnet. However, these quaternary Heusler alloys are mostly not synthesized in experiment. In 2011, Basit et al. [34] synthesized the quaternary CoFeTiAl (CFTA) alloy with LiMgPdSb-type structure and investigated the structure and the magnetic properties of CoFe_{1-x}Ti_{1-x}Al alloys in experiment. But the investigations on the detailed electronic structures and the effect of anti-site disordering on the electronic structure are absent.

In this paper, we will focus on the CFTA and mainly investigate

* Corresponding author. Building 8, 1st Road, DingZiGu Hongqiao Zone, Tianjin, PR China. Tel./fax: +86 26564070.

E-mail address: gdlui1978@126.com (G.D. Liu).

the effect of anti-site disordering on the electronic structure by first-principle calculations. A series of half-metallic diluted magnetic semiconductors generated by anti-site disordering will be predicted based on our calculated results.

2. Computational details

The Korrington–Kohn–Rostoker method combined with the coherent potential approximation and the local density approximation (KKR-CPA-LDA method) is a high-speed, high-precision and powerful method to carry out the first-principle calculations for disordered systems [35–39]. In this paper, the density of states (DOS) patterns and magnetic properties were calculated using the spin-polarized KKR-CPA-LDA method [40,41] for the CFTA alloys with various anti-site disordering. In the calculations, sixty k points in the irreducible Brillouin zone were adjusted to achieve self-consistency. The convergence tolerance is 0.1 mRy for the total energy. The muffin-tin sphere radii of 2.3 a.u. were used for all the atoms. The density of states was achieved by the tetrahedral integration method [42]. The band structures of the perfectly ordered CFTA alloy were calculated by the CASTEP package [43,44].

3. Results and discussion

The LiMgPdSb-type CFTA structure model is shown in Fig. 1. The structure is composed of four face-centered-cubic sublattices interpenetrating along the space diagonal. In the Wyckoff coordinates, Co atoms occupy the A(0,0,0) site, Fe atoms occupy the C(1/2,1/2,1/2) site, Ti atoms occupy the B(1/4,1/4,1/4) site and Al atoms occupy the D(3/4,3/4,3/4) site. We use “x% ($0 < x \leq 15$) Co–Fe anti-site” to represent the exchange of x% of Co at A sites and x% of Fe at C sites. The same expression is also applied to Co–Ti and Fe–Ti anti-site disordering. The abbreviations of C-FAD, C-TAD and F-TAD represent the Co–Fe, Co–Ti and Fe–Ti anti-site disordering, respectively. The equilibrium lattice parameter of the LiMgPdSb-type CFTA alloys with different anti-site disordering is firstly calculated by minimizing the total energy using KKR-CPA method. The ordered CFTA alloy is considered by 0% anti-site disordering. The equilibrium lattice parameter of the ordered CFTA alloy is 5.84 Å, which is slightly less than 5.85 Å obtained from the X-ray diffraction patterns measured at room temperature [34]. It is reasonable to attribute the slight difference between the theoretical and the experimental result to the measurement error or

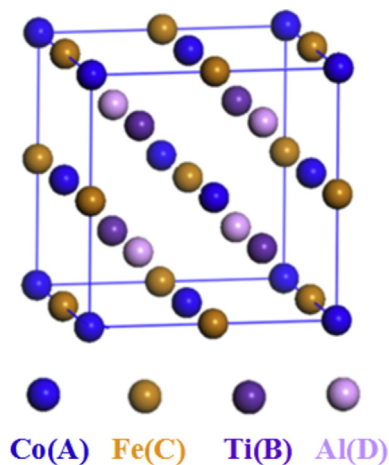


Fig. 1. Crystal structure of LiMgPdSb-type CoFeTiAl alloy. Co atoms occupy the A(0,0,0) site, Fe atoms occupy the C(1/2,1/2,1/2) site, Ti atoms occupy the B(1/4,1/4,1/4) site and Al atoms occupy the D(3/4,3/4,3/4) site.

thermal expansion. In addition, our calculated results indicate that the equilibrium lattice parameters are almost the same as for the ordered case for all the CFTA alloys with different anti-site disordering. So, the lattice parameter of 5.84 Å is used to calculate the DOS patterns, band structures and magnetic properties for all the CFTA alloys with different anti-site disordering.

In order to observe clearly the electronic properties, the CASTEP code is firstly used to calculate the band structures of the ordered LiPbMgSn-type CFTA alloy since the KKR-CPA method does not work to give the band structure. The achieved band structures are shown in Fig. 2(a). It is clear that the ordered LiPbMgSn-type CFTA alloy is a semiconductor with a direct band gap of about 0.2 eV. Fig. 2(b) shows the total DOS (TDOS) patterns calculated by CASTEP and KKR-CPA method, respectively. It can be seen that these two TDOS patterns are quite consistent in the shape and the distribution of DOS. The only difference is that the band gap width achieved by KKR-CPA method is smaller than that by CASTEP. Although these two theoretical methods are slightly different in the prediction of the band gap width, the calculated results by both these methods indicate that the ordered CFTA alloy is a semiconductor.

Fig. 3 shows the curves of the total energy versus the degree of anti-site disordering for the CFTA alloy with C-FAD, C-TAD and F-TAD. It can be seen that the total energy increases linearly with the increasing x for the CFTA alloy with F-TAD and C-TAD. The incremental intensity is 3 meV and 4.2 meV per 1%. For the C-FAD case, the total energy nonlinearly and monotonously increases with the increasing x. The incremental intensity is less than 0.12 meV per 1% in the whole calculation range, which is far less than that generated by the C-TAD and F-TAD. At the same time, the total energies of the CFTA alloys with the Co–Fe anti-site disordering are quite close to that of the ordered CFTA alloy and always lower than those with the Co–Ti and Fe–Ti anti-site disordering. These are all signs that the Co–Fe anti-site disordering is easy to occur and the Co–Ti anti-site disordering should rarely occur in the CFTA alloy.

The electronic structures of the CFTA alloys with 1–15% CFAD are calculated. Several typical DOS patterns are shown in Fig. 4(a). From Fig. 4(a), it can be seen that all the CFTA alloys with Co–Fe anti CFAD are in a nonmagnetic ground state. The DOS and the band gap near the Fermi level is hardly affected by the CFAD. More clearly, the difference of total DOS between the ordered CFTA alloy and the CFTA alloys with the CFAD are shown in Fig. 4(b). It can be seen that the difference of total DOS is almost zero in the range of 0.2 eV near the Fermi level. So, it is clear that the CFAD has no influence on the semiconductive characteristic of the ordered CFTA matrix. Since all the DOS patterns of the CFTA alloys with 1–15% CFAD are quite

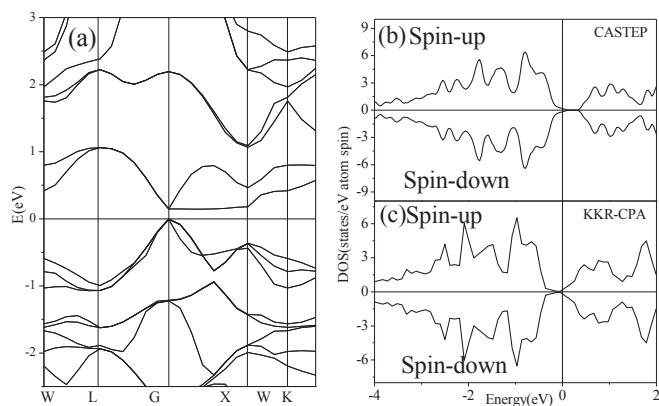


Fig. 2. (a) Band structure achieved by the CASTEP code, (b) the total DOS (TDOS) patterns achieved by the CASTEP code and (c) the TDOS patterns achieved by the KKR-CPA method for the ordered LiPbMgSn-type CoTiFeAl alloy.

Download English Version:

<https://daneshyari.com/en/article/1607357>

Download Persian Version:

<https://daneshyari.com/article/1607357>

[Daneshyari.com](https://daneshyari.com)